J Appl Electrochem (2008) 38:923–929
DOI 10.1007/s10800-008-9497-3

ORIGINAL PAPER

Anodic oxidation of mecoprop herbicide at lead dioxide

Marco Panizza · Ignasi Sirés · Glacomo Cerisola

Received: 28 July 2007 / Revised: 11 January 2008 / Accepted: 23 January 2008 / Published online: 5 February 2008

Abstract The electrochemical oxidation of an aqueous solution containing mecoprop (2-(2-methyl-4-chlorophenoxy)propionic acid) has been studied at PbO_2 anodes by cyclic voltammetry and bulk electrolysis. The influence of current density, hydrodynamic conditions, temperature and pH on the degradation rate and current efficiency is reported. The results obtained show that the use of PbO_2 leads to total mineralization of mecoprop due to the production of oxidant hydroxyl radical electrogenerated from water discharge. The current efficiency for the electrooxidation of mecoprop is enhanced by low current density, high recycle flow-rates and high temperature. In contrast, the pH effect was not significant. It has also been observed that mecoprop decay kinetics follows a pseudo-first-order reaction and the rate constant increases with rising current density.

Keywords Lead dioxide anode · Electrochemical oxidation · Mecoprop · Herbicides

1 Introduction

Herbicides are widely used in agriculture to control weeds to increase the yield of crops, in landscape turf management and also in total vegetation control programs for maintenance of highways and railroads. However, the extensive use of these substances has contributed to pollution of the environment, so residual herbicides along with their degradation byproducts have been found in surface waters, wastewaters and even in drinking waters [1]. Therefore, there is an increasing interest in reliable technologies for their removal. This is currently achieved by physico-chemical methods, such as adsorption onto activated carbon [2] and membrane filtration [3], or by chemical oxidation using single agents, including ozone [4], hydrogen peroxide or chlorine [5]. Advanced oxidation processes (AOPs), which consist of oxidant combinations as for example O_3/H_2O_2 [4], O_3/UV, UV/H_2O_2 [6], Fenton's reagent [7] and photocatalytic oxidation [8] are also proposed for the treatment of agricultural and industrial wastewaters contaminated with herbicides.

In the recent past, several papers have demonstrated that the so-called "advanced electrochemical oxidation processes", based on the direct and indirect electrogeneration of the highly oxidizing hydroxyl radical ($^{\bullet}OH$), may also be used successfully for herbicide removal. Many chlorophenoxy herbicides have been oxidized using electrogenerated Fenton's reagent [9–16]. In this technique, hydrogen peroxide is continuously generated in an acidic contaminated solution from the two-electron reduction of O_2 at RVC, carbon-felt or gas-diffusion cathodes:

$$O_2 + 2H^+ + 2e^- \rightarrow H_2O_2 \quad (1)$$

The oxidizing power of H_2O_2 is usually enhanced by addition of catalytic amounts of Fe^{2+} or Fe^{3+} to the solution, thus allowing the formation of $OH^{\bullet}$ from the well-known Fenton's reaction between Fe^{2+} and H_2O_2:

$$Fe^{2+} + H_2O_2 \rightarrow Fe^{3+} + OH^- + OH^{\bullet} \quad (2)$$

Usually, the major drawback of Fenton-based systems is the production of sludge from iron precipitation, thus requiring further disposal.

M. Panizza (✉) · I. Sirés · G. Cerisola
Department of Chemical and Process Engineering, University of Genoa, P.le J.F. Kennedy 1, 16129 Genoa, Italy
e-mail: marco.panizza@unige.it

Particularly appealing is anodic oxidation, based on the electrogeneration of hydroxyl radicals directly at the anode surface from water discharge:

$$H_2O \rightarrow (^{\bullet}OH)_{ads} + H^+ + e^- \quad (3)$$

It has been generally observed that the nature of the electrode material strongly influences the efficiency of the anodic oxidation process. While for classical anode materials, like Pt [17–19], C [20, 21] or IrO_2 [22, 23] the oxygen transfer reactions are slow and characterized by low faradaic yields and current loss due to O_2 evolution, the use of anodes with high oxygen overpotential, like PbO_2 or boron-doped diamond (BDD), favours the degradation and enhances the current efficiency.

BDD possess several technologically important characteristics including an inert surface with low adsorption properties, remarkable corrosion stability and extremely high oxygen evolution overpotential. BDD is therefore a promising material for water treatment [24]. So far, many papers have demonstrated that BDD anodes allow complete mineralization, with high current efficiency, of several types of organic compound, such as phenols [25–28], naphthol [29], carboxylic acids [30, 31], aniline [32, 33] and also various herbicides [15–17, 34–36].

However, despite the numerous advantages of diamond electrodes, they have not yet found wide industrial application, mainly due to their high cost and the difficulties in finding an appropriate substrate on which to deposit the thin diamond layer.

In contrast, PbO_2 is an inexpensive material and relatively easy to prepare, with low electrical resistivity, good chemical stability and large area, thus being optimum for wide industrial applications and in particular for the destruction of water organic pollutants [37–41]. Bonfatti et al. [19], when comparing the oxidation of glucose on different electrode materials such as Ti/PbO_2, Ti/Pt, and Ti/Pt–SnO_2, showed that the incineration of glucose and its oxidation intermediates (i.e., gluconic and glucaric acid) takes place at reasonable rate only at Ti/PbO_2 electrodes. Abaci et al. [42] observed that highly crystalline β-PbO_2 films had stronger performance on phenol degradation thanks to a porous structure that provides an enhanced active surface area, increasing the formation of $^{\bullet}OH$ and favouring the anodic oxidation process.

It has also been reported that the activity and stability of PbO_2 anodes may be significantly improved by the incorporation of dopants such as Fe^{3+}, Bi^{n+}, Co^{2+} and mixtures like Fe–F [43–45].

The aim of this work is to study the electrochemical oxidation of a concentrated solution containing the herbicide mecoprop (2-(2-methyl-4-chlorophenoxy)propionic acid, MCPP) by anodic oxidation using a PbO_2 anode. Mecoprop was chosen as a model compound because it is a selective, hormone-type chlorophenoxy acid herbicide used worldwide on a large scale for weed control on cereal crops, grasslands and lawns [46]. The influence of the main operating parameters, such as current density, recycle flow-rate, pH and temperature on COD decay and current efficiency has been investigated.

2 Experimental

The deposit of lead dioxide was made by electrochemical oxidation of an aqueous 0.1 M HNO_3 solution containing 0.5 M $Pb(NO_3)_2$ and 0.05 M NaF on titanium substrates. The titanium grid was sandblasted and chemically etched with concentrated hydrochloric acid. Lead dioxide was galvanostatically deposited using a single compartment cell and applying a current density of 20 mA cm^{-2} for 30 min [37]. In order to stabilize the electrode, a post-deposition treatment was applied to the PbO_2 films. The electrode potential was cycled in 0.5 M H_2SO_4 between 0 and 1.8 V until successive voltammetric curves were identical. SEM analysis of the electrode surface showed that the PbO_2 layer obtained after the post-treatment was continuous and crystalline with a thickness of about 200 μm.

The solutions were prepared by dissolving 320 mg L^{-1} of reagent grade MCPP ($C_{10}H_{11}ClO_3$, from Lancaster) in bidistilled water in the presence of 0.05 M Na_2SO_4 (analytical grade from Aldrich) as supporting electrolyte. The treatment of such a high MCPP concentration can make easier the identification and monitoring of the oxidation intermediates. The molecular structure of MCPP is illustrated in Fig. 1. During the experiments, pH was adjusted to the desired value by adding NaOH or H_2SO_4.

Cyclic voltammetry was carried out at 25 °C in a conventional three-electrode cell using a computer controlled EG&G potentiostat model M 273. PbO_2 was used as working electrode, a saturated calomel electrode (SCE) as a reference and a Pt wire as counter electrode. The exposed apparent area of the working electrode was 1 cm^2.

FT-IR-RAS spectra were recorded by a Nicolet Magna 750 Fourier transform spectrometer (4 cm^{-1} resolution),

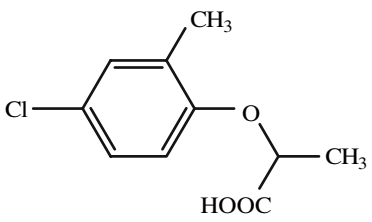

Fig. 1 Chemical structure of mecoprop (MCPP)

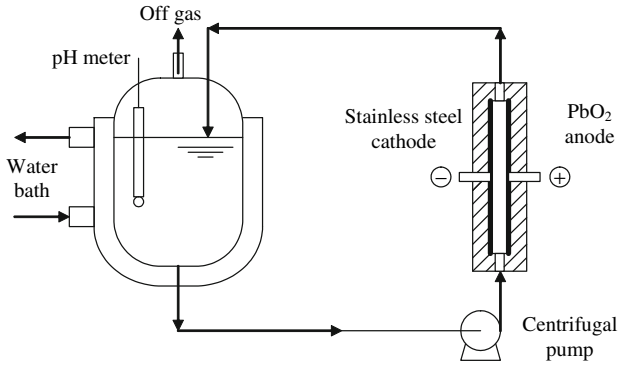

Fig. 2 Detail of the experimental setup for the anodic oxidation of MCPP

using a Specac 19700 specular reflectance accessory (angle of incidence 26.5° from normal).

The bulk oxidations of mecoprop were performed in a one-compartment electrolytic flow cell under galvanostatic conditions using an AMEL 2055 potentiostat/galvanostat (see Fig. 2). A PbO_2 grid described above was used as anode and stainless steel AISI 304 as cathode. Both electrodes had a geometric area of 50 cm^2, the interelectrode gap being 0.5 cm. The electrolyte was stored in a 450 ml thermoregulated glass reservoir and circulated through the electrolytic cell by a centrifugal pump with different recycle flow-rates in the range 75–300 L h^{-1}.

The chemical oxygen demand (COD) of the solution was monitored during electrolysis using a Dr. Lange LASA50 system. The lower detection limit of the instrument was 15 mg L^{-1} of COD. The evolution of the concentration of MCPP and its oxidation intermediates produced during the electrolytic experiments was followed by HPLC on a Shimadzu Series 6 liquid chromatograph fitted with a Supelcogel H or Bio-Rad Aminex HPX column to analyse aromatics and aliphatic carboxylics, respectively.

The instantaneous current efficiency (ICE) at a given time t was calculated from the values of the COD using the relationship [31]:

$$\mathrm{ICE} = \frac{(\mathrm{COD}_t - \mathrm{COD}_{t+\Delta t})}{8\ I\ \Delta t}\ F\ V\ \cdot 100 \qquad (4)$$

where $(\mathrm{COD})_t$ and $(\mathrm{COD})_{t+\Delta t}$ are the chemical oxygen demands at times t and $t + \Delta t$ (in g_{O_2} L^{-1}), respectively, and I is the current (A), F is the Faraday constant (96,487 C mol^{-1}) and V is the volume of the treated solution (L).

3 Results and discussion

Figure 3 shows the cyclic voltammograms obtained at the PbO_2 anode, carried out in the potential region between 1.1 and 2.0 V vs. SCE in order to avoid the reduction and oxidation of Pb^{4+}/Pb^{2+}. The voltammogram in the absence of pollutant, performed in 0.05 M Na_2SO_4 (dotted line), is nearly featureless. In contrast, during the first scan (curve 1) in the presence of MCPP, a broad, ill-defined anodic peak corresponding to MCPP oxidation is observed at 1.6 V vs. SCE.

As the number of cycles increases (curves 2–5), the anodic peak for MCPP oxidation rapidly decreases until a steady state is reached after about five cycles, as clearly shown in the inset panel of Fig. 3. This decrease in electrode activity is caused by the deposition of polymeric adhesive oxidation products on the electrode surface. The presence of the polymeric film was also confirmed by FT-IR analysis of the electrode surface. Similar behaviour for the anodic oxidation of aromatics on PbO_2 [47], Pt [48] and BDD [26, 29] anodes has been reported.

However, it has been found that the PbO_2 surface regains its former activity by simple polarization at high anodic potential ($E > 2.2$ V vs. SCE) in the region of water decomposition, due to the destruction of the polymeric film responsible for the anode fouling. i.e. the i_{peak} value observed for cycle 1 can be reproduced. In fact, it has been demonstrated [49, 50] that, during water oxidation, anodes with high oxygen evolution overpotential such as PbO_2 make it possible to produce adsorbed hydroxyl radicals from reaction (5) that oxidize the polymeric deposit formed on their surface, as indicated in reaction (6):

$$PbO_2 + H_2O \rightarrow PbO_2(^{\bullet}OH)_{ads} + H^+ + e^- \qquad (5)$$

$$\text{Organic film} + PbO_2(^{\bullet}OH)_{ads} \rightarrow PbO_2 + CO_2 + H_2O \qquad (6)$$

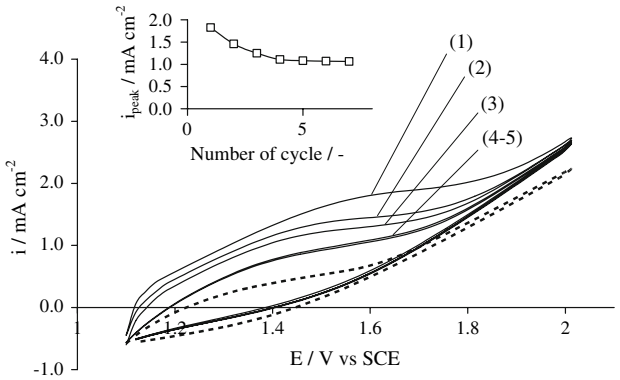

Fig. 3 Consecutive cyclovoltammograms of PbO_2 in the presence of 320 mg L^{-1} of MCPP (500 mg L^{-1} COD) in 0.05 M Na_2SO_4: consecutive cycles 1; 2; 3; 4; 5. Dotted line: background curve in 0.05 M Na_2SO_4. Scan rate 100 mV s^{-1}, $T = 25$ °C. The dependence of density current peak at 1.6 V as a function of the number of cycles is shown in the inset

Once it was well established that electrode reactivation can be obtained only in the potential region of water discharge, bulk electrolyses of MCPP solutions were carried out at current densities within this potential region. Thus, the anodic oxidation of synthetic wastewater was performed under different current densities (20–60 mA cm_{-2}), recycle flow-rates (75–300 L h_{-1}), pH values (3–8) and temperatures (25–50 °C) in order to find the best operating conditions.

Figure 4 shows the trend of the COD and current efficiency (inset) with time during the anodic oxidation of 320 mg L^{-1} of MCPP at different current densities. For all the applied currents, the COD decreases up to the detection limit (about 15 mg L^{-1}), indicating complete herbicide mineralization (>97% COD removal) from overall reaction (7) by means of its reaction with adsorbed $OH^{\bullet}$ electrogenerated on the PbO_2 surface from water discharge.

$$C_{10}H_{11}C1O_3 + 17H_2O \rightarrow 10CO_2 + C1^- + 45H^+ + 44e^- \quad (7)$$

where 44F are required to destroy each mol of MCPP.

It can also be observed that the oxidation rate (i.e., dCOD/dt) increases slightly with rising current, meaning that in such conditions of high recycle flow-rate (e.g. 300 L h^{-1}) and high organic loading (320 mg L^{-1} of MCPP), the oxidation is carried out at a current below the limiting. Therefore, the process is under charge transfer control because a greater charge passing into the cell favours the oxidation of the pollutant and its intermediates. However, increasing current density results in a lower current efficiency (Fig. 4, inset) and, consequently, in an increasing specific charge for total mineralization, due to a relative greater amount of $PbO_2(^{\bullet}OH)_{ads}$ wasted in parasite non-oxidizing reactions such as oxygen evolution:

$$2PbO_2(^{\bullet}OH)_{ads} \rightarrow 2PbO_2 + O_2 + 2H^+ + 2e^- \quad (8)$$

The decay of MCPP concentration during the electrolyses at different current densities was followed by reversed-phase HPLC and the results are reported in Fig. 5. MCPP disappears after 110, 210 and 300 min of anodic oxidation at 60, 40 and 20 mA cm^{-2}, respectively, in good agreement with the lower production of hydroxyl radicals as current density decreases. All the MCPP concentration decays could be very satisfactorily described by a pseudo-first-order kinetics (Fig. 5, inset):

$$-\frac{d[MCPP]}{dt} = k_{app} \cdot [MCPP] \quad (9)$$

which can be integrated to give the following expression:

$$\ln\frac{[MCPP]_0}{[MCPP]_t} = k_{app} \cdot t \quad (10)$$

where $[MCPP]_0$ and $[MCPP]_t$ are the concentration of MCPP at the beginning and at time t, and k_{app} is the apparent observed pseudo-first-order rate constant. From this analysis it was found that the pseudo-first-order rate constant increases from 2.1×10^{-4} s^{-1} to 3.2×10^{-4} s^{-1} and 6.3×10^{-4} s^{-1} with increasing current from 20 to 40 and 60 mA cm^{-2}, respectively.

By comparing the results reported in Figs. 4 and 5, it is worth noting that MCPP is removed more rapidly than the COD of the solution, meaning that some oxidation intermediates are formed. Aromatic products such as 4-chloro-*o*-cresol and 2-methyl-*p*-benzoquinone, and aliphatic carboxylic acids such as maleic, pyruvic, acetic and oxalic acids have been identified as the main intermediates. These findings fit very well with the results of Flox et al. [36] using a BDD anode for the anodic oxidation of MCPP. These products have been quantified by reversed-phase or ionic-exclusion HPLC, and Fig. 6 shows the influence

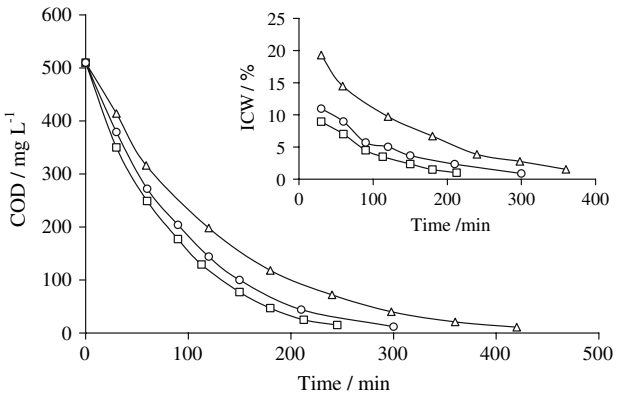

Fig. 4 Influence of current density on the evolution of COD and ICE (inset) with time during the electrolyses of 320 mg L^{-1} of MCPP in 0.05 M Na_2SO_4 using the PbO_2 anode. Recycle flow-rate = 300 L h^{-1}; T = 25 °C; pH = 3; applied current density (i): (Δ) 20 mA cm^{-2}; (◯) 40 mA cm^{-2}; (□) 60 mA cm^{-2}

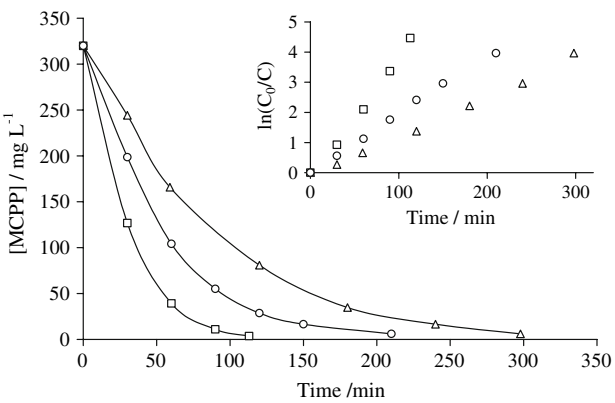

Fig. 5 MCPP decay with time for the experiments of Fig. 4. The inset panel shows its kinetics analysis assuming that the herbicide follows a pseudo-first-order reaction

of the current density on their evolution, expressed as mg of carbon L^{-1}. At higher current density, larger amounts of intermediates are accumulated in the medium, since MCPP cleavage is accelerated by reaction with more hydroxyl radicals, but they remain a shorter time in the solution due to the quicker ring opening of aromatics and the progressive oxidation of aliphatic carboxylics released. These results are in agreement with those obtained by Tahar and Savall for phenol oxidation at PbO_2 anode [41].

The influence of the recycle flow-rate on COD removal during MCPP oxidation with PbO_2 anodes at 40 mA cm^{-2} is shown in Fig. 7. The overall COD depletion is lower as the recycle flow-rate is diminished, thus meaning that at low recycle flow-rate the oxidation becomes a diffusion-controlled process. In fact, the increase in the recycle flow-rate accelerates the transport of organics towards the electrode surface, where they react with the electrogenerated hydroxyl radicals and, consequently, they disappear from the solution more quickly and with higher current efficiency (Fig. 7, inset).

Many studies have reported the effect of solution pH during anodic oxidation of organics on PbO_2 anodes, but the results are contradictory. For example, Kirk et al. [51] showed that the current efficiency for the oxidation of aniline increased from 3% to 13% as pH increased from 2.0 to 11.0. However, Samed et al. [52] observed that the oxidation kinetics for 4-chloroguaiacol removal was faster at pH 2.0 than at pH 6.0. These discrepancies can be accounted for by the differences in the chemical properties of the organic tested. In order to study the influence of pH during the oxidation of MCPP, some electrolyses were carried out at three initial pH values in the range 3.0–8.0, and the results are shown in Fig. 8. COD removal was almost unaffected by solution pH, achieving complete

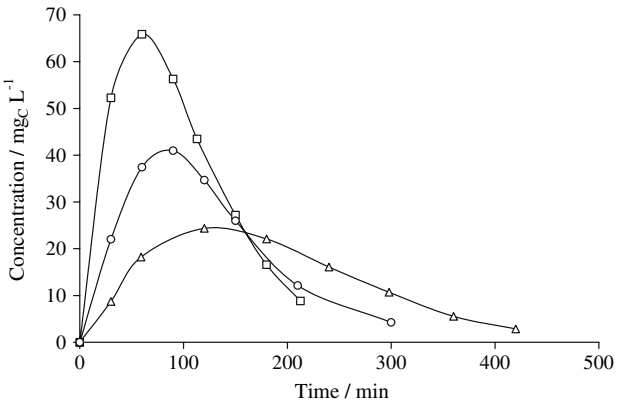

Fig. 6 Time-evolution of the reaction intermediates, expressed as mg_C L^{-1}, during the anodic oxidation of 320 mg L^{-1} of MCPP in 0.05 M Na_2SO_4 using the PbO_2 anode at different current density values. Recycle flow-rate = 300 L h^{-1}; T = 25 °C; pH = 3; i: (Δ) 20 mA cm^{-2}; (◯) 40 mA cm^{-2}; (□) 60 mA cm^{-2}

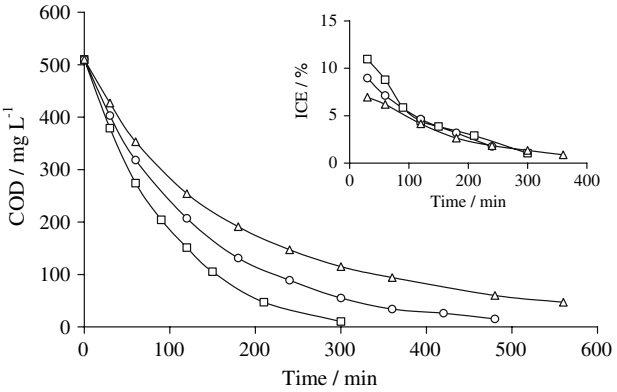

Fig. 7 Effect of recycle flow-rate on the COD evolution during the anodic oxidation of 320 mg L^{-1} of MCPP in 0.05 M Na_2SO_4 using the PbO_2 anode. T = 25 °C; pH = 3; i = 40 mA cm^{-2}; recycle flow-rate: (Δ) 75 L h^{-1}; (◯) 200 L h^{-1}; (□) 300 L h^{-1}

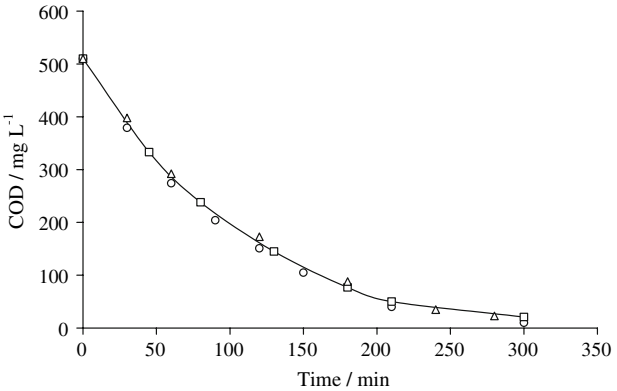

Fig. 8 Influence of solution pH on the evolution of COD with time during the electrolyses of 320 mg L^{-1} of MCPP in 0.05 M Na_2SO_4 using the PbO_2 anode. Recycle flow-rate = 300 L h^{-1}; T = 25 °C; i = 40 mA cm^{-2}; pH: (◯) 3; (Δ) 5; (□) 8

mineralization (i.e. 97% of COD removal) in 300 min in all cases.

The oxidation of MCPP was also carried out at different temperatures by strictly thermostating the system. The variation of the COD and MCPP concentration during the electrolysis at 25, 40 and 50 °C when applying a current density of 40 mA cm^{-2} and with a recycle flow-rate of 300 L h^{-1} is presented in Fig. 9. Increase in temperature favours both COD and MCPP removal. This is in agreement with other studies for the oxidation of organics [19, 41, 52]. This behaviour can be explained in terms of the electrogeneration of inorganic oxidizing agents. In fact, it has been demonstrated [53] that ozone, and also small amount of hydrogen peroxide, can be formed during electrolyses with PbO_2 electrodes at high potentials:

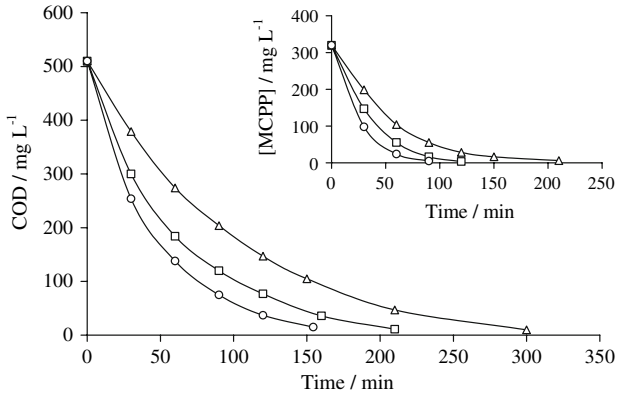

Fig. 9 Effect of temperature on the evolution of COD and MCPP concentration with time during the electrolyses of 320 mg L^{-1} of MCPP in 0.05 M Na_2SO_4 using the PbO_2 anode. Recycle flow-rate = 300 L h^{-1}; i = 40 mA cm^{-2}; T: (Δ) 25 °C; (□) 40 °C; (◯) 50 °C

Table 1 Effect of electrolysis temperature on the pseudo-first-order rate constants for MCPP oxidation under conditions given in Fig. 9

Temperature/°C	$k_{app} \times 10^4/s^{-1}$
25	3.22
40	5.23
50	7.48

$$PbO_2(OH^{\bullet})_{ads} \rightarrow PbO_2(O^{\bullet})_{ads} + H^+ + e^- \quad (11)$$

$$PbO_2(O^{\bullet})_{ads} + O_2 \rightarrow PbO_2 + O_3 \quad (12)$$

These reagents are known to be powerful oxidants that can act as mediators for organics oxidation. The oxidation rate of organic compounds with ozone, hydrogen peroxide and all the oxidants as a whole increases with temperature, as demonstrated by Flox et al. for anodic oxidation with Pt and BDD [17]. In addition, since the diffusion rate increases with rising temperature due to the decrease in the medium viscosity, an increase in temperature can bring about a slight increase in the degradation rate, leading to a further reduction in the residual COD. The values of the pseudo-first-order rate constants for MCPP oxidation at different temperatures, which were calculated from the slopes of Fig. 9 (inset) using Eq. 10, are reported in Table 1. They increase with temperature, and the activation energy value, calculated using Arrhenius's Law, is 26.6 kJ mol^{-1}.

4 Conclusion

The electrochemical oxidation of the herbicide mecoprop in aqueous solution has been investigated by anodic oxidation at PbO_2 anode under different experimental conditions, i.e., applied current, recycle flow-rate, pH and temperature. The results reveal the following traits:

- A polymeric film, which causes electrode fouling, is formed during mecoprop oxidation in the potential region of water stability. However, it is removed by high-potential anodic polarization in the region of water discharge.
- In the range studied, within the water oxidation domain, the total mineralization (>97% COD abatement) of MCPP is obtained, regardless of the operating conditions, due to the formation of hydroxyl radicals coming from the water discharge.
- Mecoprop decay kinetics follow a pseudo-first-order reaction, and the rate constant increases with current density.
- An increase in liquid recycle flow rate and temperature accelerates the COD removal and enhances the current efficiency.
- The pH effect on the degradation rate is not significant.

Acknowledgements I.S. acknowledges the support from the members of the Laboratorio di Elettrochimica, Corrosione e Protezione dei Materiali Metallici of the Università degli Studi di Genova to draw up this paper.

References

1. Barbash JE, Thelin GP, Kolpin DW, Gilliom RJ (2001) J Environ Qual 30:831–845
2. Kim T-Y, Kim S-J, Cho S-Y (2005) Adsorption 11:217–221
3. Bonne PAC, Beerendonk EF, van der Hoek JP, Hofman JAMH (2000) Desalination 132:189–193
4. Acero JL, Benitez FJ, Real FJ, Maya C (2003) Ind Eng Chem Res 42:5762–5769
5. Acero JL, Real FJ, Benitez J, Gonzalez M (2007) J Chem Technol Biotechnol 82:214–222
6. Benitez FJ, Acero JL, Real FJ, Roman S (2004) J Environ Sci Health B 39:393–409
7. Rivas FJ, Navarrete V, Beltrán FJ, García-Araya JF (2004) Appl Catal B: Environ 48:249–258
8. Konstantinou IK, Sakkas VA, Albanis TA (2001) Appl Catal B: Environ 34:227–239
9. Badellino C, Rodrigues CA, Bertazzoli R (2007) J Appl Electrochem 37:451–459
10. Badellino C, Rodrigues CA, Bertazzoli R (2006) J Hazard Mater 137:856–864
11. Boye B, Dieng MM, Brillas E (2002) Environ Sci Technol 36:3030–3035
12. Oturan MA (2000) J Appl Electrochem 30:475–482
13. Brillas E, Boye B, Dieng MM (2003) J Electrochem Soc 150:583–589
14. Brillas E, Baños MA, Garrido JA (2003) Electrochim Acta 48:1697–1705
15. Brillas E, Baños MA, Skoumal M, Cabot PL, Garrido JA, Rodríguez RM (2007) Chemosphere 68:199–209
16. Brillas E, Boye B, Sirés I, Garrido JA, Rodríguez RM, Arias C, Cabot PL, Comninellis C (2004) Electrochim Acta 49:4487–4496

17. Sirés I, Cabot PL, Centellas F, Garrido JA, Rodríguez RM, Arias C, Brillas E (2006) Electrochim Acta 52:75–85
18. Comninellis C (1994) Electrochim Acta 39:1857–1862
19. Bonfatti F, Ferro S, Lavezzo F, Malacarne M, Lodi G, De Battisti A (1999) J Electrochem Soc 146:2175–2179
20. Polcaro AM, Palmas S, Renoldi F, Mascia M (2000) Electrochim Acta 46:389–394
21. Awad YM, Abuzaid NS (1999) Sep Sci Technol 34:699–708
22. Foti G, Gandini D, Comninellis C, Perret A, Haenni W (1999) Electrochem Solid State Lett 2:228–230
23. Pulgarin C, Adler N, Peringer P, Comninellis C (1994) Water Res 28:887–893
24. Panizza M, Cerisola G (2005) Electrochim Acta 51:191–199
25. Iniesta J, Michaud PA, Panizza M, Cerisola G, Aldaz A, Comninellis C (2001) Electrochim Acta 46:3573–3578
26. Rodrigo MA, Michaud PA, Duo I, Panizza M, Cerisola G, Comninellis C (2001) J Electrochem Soc 148:D60-D64
27. Cañizares P, Díaz M, Domínguez JA, García-Gómez J, Rodrigo MA (2002) Ind Eng Chem Res 41:4187–4194
28. Cañizares P, García-Gómez J, Sáez C, Rodrigo MA (2003) J Appl Electrochem 33:917–927
29. Panizza M, Michaud PA, Cerisola G, Comninellis C (2001) J Electroanal Chem 507:206
30. Gandini D, Mahé E, Michaud PA, Haenni W, Perret A, Comninellis C (2000) J Appl Electrochem 30:1345–1350
31. Cañizares P, García-Gómez J, Lobato J, Rodrigo MA (2003) Ind Eng Chem Res 42:956–962
32. Mitadera M, Spataru N, Fujishima A (2004) J Appl Electrochem 34:249–254
33. Polcaro AM, Mascia M, Palmas S, Vacca A (2004) Electrochim Acta 49:649–656
34. Sirés I, Centellas F, Garrido JA, Rodríguez RM, Arias C, Cabot PL, Brillas E (2007) Appl Catal B: Environ 72:373–381
35. Boye B, Brillas E, Marselli B, Michaud P-A, Comninellis C, Farnia G, Sandona G (2006) Electrochim Acta 51:2872–2880
36. Flox C, Cabot PL, Centellas F, Garrido JA, Rodríguez RM, Arias C, Brillas E (2006) Chemosphere 64:892–902
37. Panizza M, Cerisola G (2004) Environ Sci Technol 38:5470–5475
38. Polcaro AM, Palmas S, Renoldi F, Mascia M (1999) J Appl Electrochem 29:147–151
39. Kawagoe KT, Johnson DC (1994) J Electrochem Soc 141:3404–3409
40. Tahar NB, Savall A (1999) J Appl Electrochem 29:277–283
41. Tahar NB, Savall A (1998) J Electrochem Soc 145:3427–3434
42. Abaci S, Tamer U, Pekmez K, Yildiz A (2005) Appl Surf Sci 240:112–119
43. Andrade LS, Ruotolo LAM, Rocha-Filho RC, Bocchi N, Biaggio SR, Iniesta J, García-García V, Montiel V (2007) Chemosphere 66:2035–2043
44. Treimer SE, Feng JR, Scholten MD, Johnson DC, Davenport AJ (2001) J Electrochem Soc 148:E459
45. Velichenko AB, Amadelli R, Baranova EA, Girenko DV, Danilov FI (2002) J Electroanal Chem 527:56–64
46. Thomson WT (1982) Agricultural chemicals book II herbicides. Thomson Publications, Fresno
47. Panizza M, Cerisola G (2003) Electrochim Acta 48:3491–3497
48. Rodgers JD, Jedral W, Bunce NJ (1999) Environ Sci Technol 33:1453–1457
49. Cong Y, Wu Z (2007) J Phys Chem C 111:3442–3446
50. Ai S, Wang Q, Li H, Jin L (2005) J Electroanal Chem 578:223–229
51. Kirk DW, Sharifian H, Foulkes FR (1985) J Appl Electrochem 15:285–292
52. Samet Y, Elaoud SC, Ammar S, Abdelhedi R (2006) J Hazard Mater 138:614–619
53. Amadelli R, De Battisti A, Girenko DV, Kovalyov SV, Velichenko AB (2000) Electrochim Acta 46:341–347